Observation of Parametric Instability in Advanced LIGO

Matthew Evans,* Slawek Gras, Peter Fritschel, John Miller, and Lisa Barsotti
Massachusetts Institute of Technology, Cambridge, MA 02139, USA

Denis Martynov, Aidan Brooks, Dennis Coyne, Rich Abbott, Rana Adhikari, Koji Arai, Rolf Bork, Bill Kells, Jameson Rollins, Nicolas Smith-Lefebvre, Gabriele Vajente, and Hiroaki Yamamoto
California Institute of Technology, Pasadena, CA 91125, USA

Ryan Derosa, Anamaria Effler, and Keiko Kokeyama
Louisiana State University, Baton Rouge, LA 70803, USA

Carl Adams, Stuart Aston, Joseph Betzweiser, Valera Frolov, Matthew Heinze, Adam Mullavey, Arnaud Pele, Janeen Romie, Michael Thomas, and Keith Thorne
LIGO Livingston Observatory, Livingston, LA 70754, USA

Sheila Dwyer, Kiwamu Izumi, Keita Kawabe, and Daniel Sigg
LIGO Hanford Observatory, Richland, WA 99352, USA

Stefan Ballmer and Thomas J. Massinger
Syracuse University, Syracuse, NY 13244, USA

Alexa Staley
Columbia University, New York, NY 10027, USA

Chris Mueller
University of Florida, Gainesville, FL 32611, USA

Hartmut Grote
Max Planck Institute for Gravitational Physics, 30167 Hannover, Germany

Robert Ward
Australian National University, Canberra, ACT 0200, Australia

Eleanor King
University of Adelaide, Adelaide, SA 5005, Australia

David Blair, Li Ju, and Chunnong Zhao
University of Western Australia, Crawley WA 6009, Australia

(Dated: March 4, 2022)

Parametric instabilities have long been studied as a potentially limiting effect in high-power interferometric gravitational wave detectors. Until now, however, these instabilities have never been observed in a kilometer-scale interferometer. In this work we describe the first observation of parametric instability in an Advanced LIGO detector, and the means by which it has been removed as a barrier to progress.

arXiv:1502.06058v2 [astro-ph.IM] 27 Feb 2015

INTRODUCTION

Opto-mechanical interactions, the moving of masses by radiation pressure, are typically of such a tenuous nature that even carefully designed experiments may fail to observe them. In the extreme environment of a high-power interferometric gravitational wave detector, however, these effects arise spontaneously. This is true despite the fact that these instruments feature multi-kilogram optics [1], unlike the micro-gram or nano-gram optics generally used in experiments which target such effects [2–5].

Since the seminal work of Braginsky, Strigin, and Vyatchanin in 2001 [6], optical parametric instabilities have been extensively studied as a potential limit to high-power operation of interferometric gravitational wave detectors [7–35]. These instabilities are of acute interest because, if left unchecked, they will limit detector sensitivity by limiting circulating power.

We report on the first observation of a self-sustaining parametric instability in a gravitational wave detector and the subsequent quenching of this instability. This observation, at the LIGO Livingston Observatory (LLO) [36], the culmination of more than a decade of the-

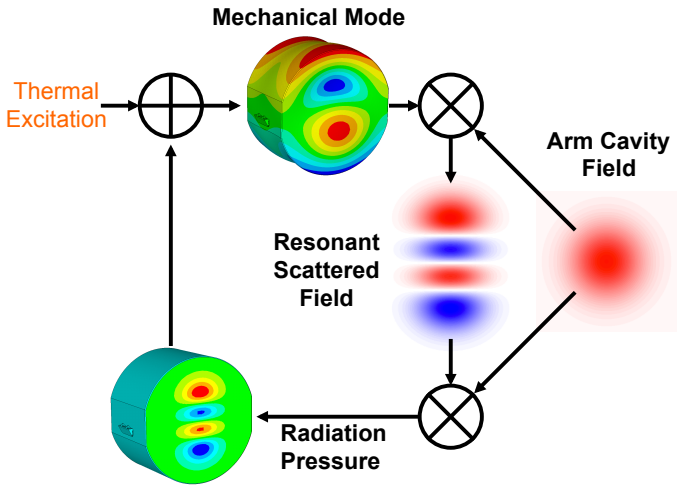


FIG. 1. Parametric instabilities transfer energy from the arm cavity field to a mechanical mode of an interferometer test mass. Since the rate of energy transfer depends on the amplitude of the excited mechanical mode, this can be a runaway positive feedback process.

oretical calculation, numerical modeling, and lab-scale experimentation, and serves as confirmation that models which have been built to understand the phenomenon of parametric instability are substantially correct.

A variety of techniques have been suggested for overcoming parametric instabilities in gravitational wave detectors [37–43]. There are a few notable categories of mitigation techniques: avoid instability by changing the radius of curvature of one or more optics [37, 43], actively damp mechanical modes as they become excited [42], and prevent instability by increasing the loss of the test mass mechanical modes [29, 39, 40, 44]. The first of these techniques has been demonstrated and found to be effective at LLO.

THEORY OF PARAMETRIC INSTABILITY

Parametric instabilities (PI) operate by transferring energy from the fundamental optical mode of the interferometer, which with nearly 1 MW of circulating power can be as much as 40 J, into an interferometer optic's mechanical mode (see figure 1). Energy transfer takes place via the radiation pressure driven opto-mechanical interaction and the modulation of the fundamental field by the excited mechanical mode [25] (see figure 1).

The parametric gain for a given test mass mechanical mode is given by

$$R_m = \frac{8\pi Q_m P_{\rm arm}}{M\omega_m^2\, c\, \lambda} \sum_{n=0}^{\infty} \Re[G_n] B_{m,n}^2 \qquad (1)$$

(using the notation of reference [25], and correcting an error therein [45]). The fixed parameters used in equation 1 are: c is the speed of light, λ the laser wavelength, M the mass of the optic, ω_m the angular resonant frequency of mechanical mode with index m, and $B_{m,n}$ the overlap between mechanical mode m and optical mode n.

Clearly, the potential for instability grows with increasing power, since the parametric gain of all modes is proportional to the power circulating in the interferometer arm cavities, $P_{\rm arm}$. Active and passive damping techniques for defusing PI operate by reducing the Q of an otherwise unstable mechanical mode, while avoidance techniques work by changing the optical gain G_n to prevent instability.

The e-fold growth time for an unstable mode is given by

$$\tau_m = \frac{2Q_m}{\omega_m(R_m - 1)} \qquad (2)$$

Note that for $R_m = 0$ this gives a negative value equal to the usual decay time of a mechanical mode with frequency $f_m = \omega_m/2\pi$ and quality factor Q_m. For values of $R_m > 1$ equation 2 gives a positive value, indicating exponential growth.

The circulating power level $P_{\rm arm}$ at which a mode becomes unstable is referred to as the threshold power $\bar{P}_m$ for that mode, and is found by rearranging equation 1 with $R_m = 1$ and $P_{\rm arm} = \bar{P}_m$. At threshold the opto-mechanical interaction is putting energy into the mode at the same rate that it is being dissipated, so $\tau_m \to \infty$.

OBSERVED PARAMETRIC INSTABILITY

Parametric instability was first observed in the Advanced LIGO detector recently installed at LLO (see reference [46] for detailed information about the detectors). The instability grew until it polluted the primary gravitational wave output of the detector by aliasing into the detection band and saturating detection electronics (see figure 2). The time scale for growth was long enough to allow for manual intervention (a reduction of the laser power input to the interferometer) before control was lost due to this saturation of the readout electronics.

The test mass (TM) mechanical mode responsible for the instability was identified as the 15.54 kHz mode shown in figure 3. The higher-order mode spacing of the Advanced LIGO arm cavities is 5.1 ± 0.3 kHz, and the optical resonance width is 80 Hz, such that a $3^{\rm rd}$ order transverse optical mode can provide energy transfer from the fundamental optical mode to this mechanical mode (see figure 1 and 3).

By measuring the e-folding growth and decay time of the excited acoustic mode as a function of circulating power in the interferometer arm cavities, we can compute the parametric gain R and mechanical mode quality factor Q as given in equation 2. Our measurements were performed by operating the interferometer above

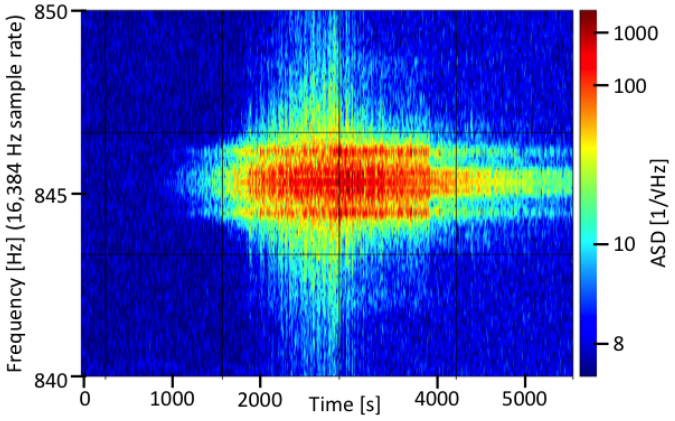


FIG. 2. The excitation due to parametric instability was first observed as an exponentially growing feature in the detector's primary output (the gravitational wave channel). The feature is aliased into the detector band by the 16 384 Hz sample rate of the digital system which causes it to appear at 845 Hz. The growing instability eventually causes saturation of the electronic readout chain, which appears as broadband contamination of the detector output channel (visible between 2500 and 3000 s). In the above data, the power into the interferometer was decreased before saturation caused the interferometer control systems to fail (see figure 4).

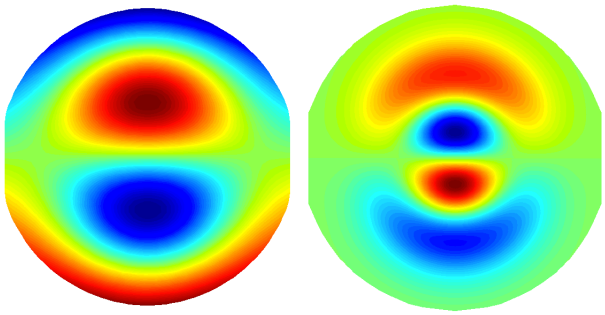


FIG. 3. The test mass mechanical mode and cavity optical mode responsible for the observed parametric instability are shown. The left panel is the test mass front surface displacement due to the mechanical mode, while the right panel is the radiation pressure induced displacement (red is positive and blue negative in both panels). Both of these modes occur at 15.5 kHz and they have an overlap factor of $B_{m,n} = 0.1$.

the threshold power to excite the TM mechanical mode and then reducing the power below the instability threshold and watching the mode amplitude decrease, as shown in figure 4.

The observed unstable mode has $R = 2$ with $P_{\rm arm} = 50\,{\rm kW}$, and the associated mechanical mode has $Q = 12 \times 10^6$. This Q-factor is in the range expected given similar measurements of Advanced LIGO test masses [42, 47], and the parametric gain is as predicted by equation 1 for a high, but far from maximal value of G_n. While the 90% confidence limit for this mode is $R = 11$, as seen in figure 5, 5% of simulated values are higher than the observed value, and 1% have $R > 100$.

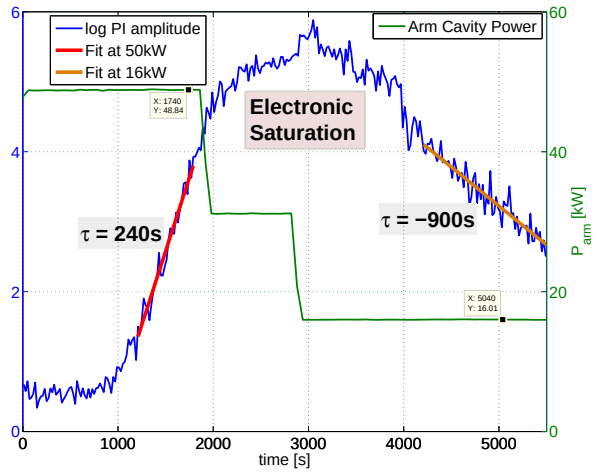


FIG. 4. The amplitude of the excitation shown in figure 2 is fitted at times with different values of $P_{\rm arm}$ to find its growth (or decay) time-scale as a function of power. The growth of the PI is clearly visible above the noise after 1000 s, with an e-folding growth time of 240 s, until 2000 s at which point the readout electronics begin to saturate. A little more than 4000 s into the plotted data, the excited mechanical mode is seen decaying with $\tau = -900\,{\rm s}$. According to equation 2, these data imply a threshold power of 25 kW and $Q = 12 \times 10^6$ for this mode.

DEFUSING PARAMETRIC INSTABILITY

Parametric instability depends on several potentially modifiable features of a gravitational wave detector, two of which can be taken advantage of in Advanced LIGO without modifications to the interferometer core optics. First, instability requires coincident resonant frequencies of a test mass mechanical mode and an arm cavity optical mode (i.e., G_n in equation 1 must be large at the mechanical mode frequency ω_m for an optical mode with non-vanishing overlap $B_{m,n}$).

The coincidence of resonant frequencies can be modified by changing the radius of curvature (RoC) of one of the test masses in the cavity affected by PI, through its effect on the transverse mode spacing. Advanced LIGO arm cavities use mirrors with $\sim 2\,{\rm km}$ RoC, so for the 3rd order optical mode shown in figure 3, for instance, a change of 1 m is sufficient to change its resonant frequency by 80 Hz, or one cavity line width.

A second approach to defusing PI comes from the weak radiation pressure coupling of energy from the fundamental optical mode to the mechanical modes of the test mass, which must be sufficient to overcome the energy loss from the mechanical mode. This can be seen in the linear dependence of R_m on Q_m in equation 1. The quality factor of mechanical modes in the Advanced LIGO test mass optics is roughly 10^7, and as such is easily spoiled. Since the highest parametric gain likely to be seen in Advanced LIGO is ~ 10, reducing Q_m to less than 10^6 for potentially unstable modes would suffice (see fig-

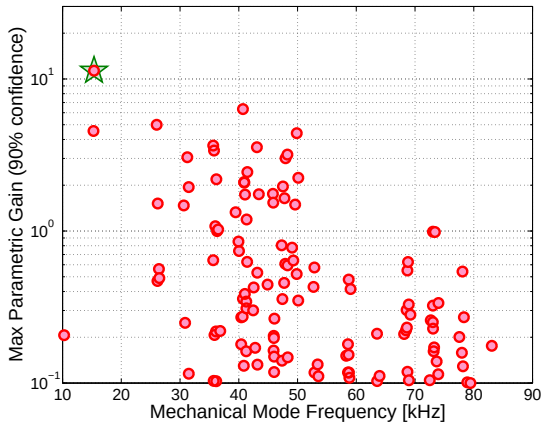


FIG. 5. The maximum gain expected at full power, $P_{\rm arm} = 800\,{\rm kW}$, for all potentially unstable modes (90% confidence value for a single test mass). Since the mechanical mode frequencies and optics parameters are known with limited precision, the parametric gain of a particular mode cannot be computed exactly, and Monte Carlo methods must be used [25]. The "90% confidence maximum" shown here is the value for which 90% of the 342,881 Monte Carlo computations gave a lower gain. Notably, the observed unstable mode is the mode with the highest predicted parametric gain (marked with a green star), and the observed gain is about a factor of 3 higher than the value shown here ($R = 2$ at 50 kW, or $R = 32$ at 800 kW). This is not so much bad luck as a trials factor; there are 4 test masses, and many potentially unstable modes, so it is not unusual that at least one is above the 90% confidence limit. In fact, the statistics shown in figure 7 confirm that the observation of at least one unstable mode was to be expected.

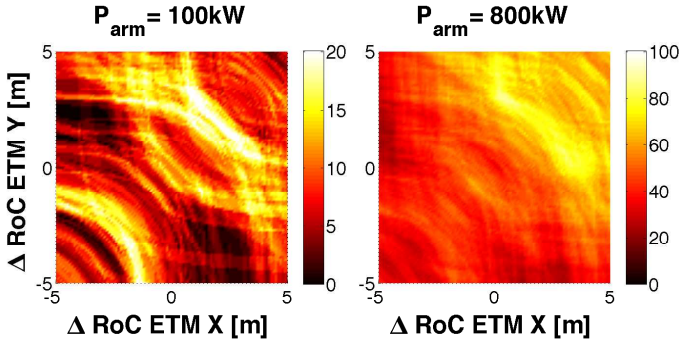


FIG. 6. The number of unstable modes as a function of change in arm cavity mirror radius of curvature (RoC), as indicated by the color scale to the right of each plot. With 100 kW of circulating power, as expected for the first observing run, small changes in mirror RoC can be used to avoid parametric instability. Higher power levels, however, increase parametric gain; note the different color scales used on the left and right panels. At Advanced LIGO's design operating power of $P_{\rm arm} = 800\,{\rm kW}$ RoC adjustments can at best be used to reduce the number of unstable modes.

ure 5).

In anticipation of PI, all Advanced LIGO test masses were outfitted with electro-static actuators capable of damping mechanical modes associated with PI [42]. This method of damping TM mechanical modes was demonstrated at MIT with a prototype Advanced LIGO optic, and will be used to damp PI in Advanced LIGO as necessary.

As discussed in the following section, the combination of the above techniques will likely prove sufficient if a manageable number of unstable modes are encountered. If, however, the number of unstable modes is very large, a broadband reduction of mechanical Q-factors may be required. Implementing a broadband PI control strategy, as described in [47], will certainly prove successful, but it may cause some delay in the approach of Advanced LIGO to its design operating power.

IMPLICATIONS FOR THE FUTURE OF ADVANCED LIGO

Shortly after the first PI was observed at LLO, heating elements, known as "ring heaters", were used to change the mirror RoC and avoid the instability. Ring heaters were included in the Advanced LIGO design to compensate for RoC changes due to absorption of the fundamental optical mode, and can change the RoC of the optics by several 10s of meters. After adjusting the ring heaters to produce roughly 2 m of RoC change of the arm-cavity end mirrors, the parametric gain of the observed instability at 15.53 kHz was reduced below unity and the interferometer was operated with nearly 100 kW of circulating power for more than 12 hours.

Despite this success, it must be recognized that many mechanical modes of the interferometer test masses can be driven to instability; figure 5 shows the maximum expected parametric gain of all potentially unstable modes. From the left panel of figure 6, we can conclude that using the ring heaters to find a PI-free zone is likely to succeed at present (with $P_{\rm arm} \sim 100\,{\rm kW}$), but the right panel tells us that at the design value of $P_{\rm arm} = 800\,{\rm kW}$ RoC changes will not be sufficient.

Several major periods of data taking are expected with Advanced LIGO at power levels below the design power [48]. Figure 7 shows the number of modes that are likely to be unstable as a function of circulating power in the interferometer. At the final operating power, for instance, more than 40 modes are likely to be unstable.

In order to operate at the design power level Advanced LIGO will likely need to employ multiple methods of defusing PI: changing the RoC to reduce the number of unstable modes; actively damping the remaining unstable modes with electrostatic actuators; and possibly reducing the Q of the test mass modes with passive dampers.

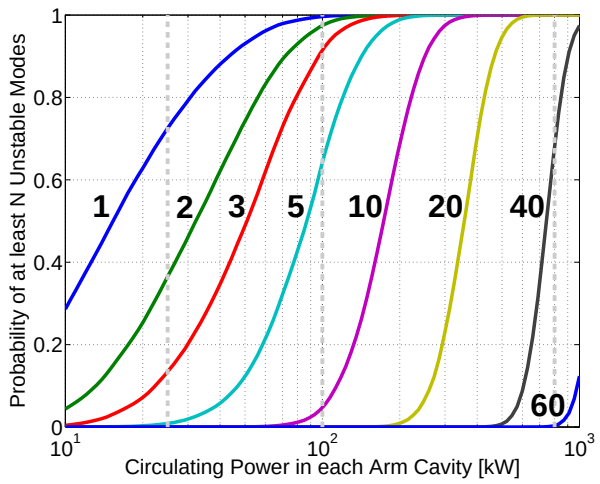


FIG. 7. The probabilities of having various numbers of unstable modes anywhere in the interferometer (with 4 test masses), as a function of circulating power, $P_{\rm arm}$. Each curve gives the probability that at least $N = \{1, 2, 3, 5, \ldots\}$ unstable modes are observed in an Advanced LIGO interferometer at a given level of circulating power in the arm cavities. The vertical grey lines mark the threshold power of the mode first observed to be unstable, near 25 kW of circulating power, the power level at which the first observing run of Advanced LIGO is planned, roughly 100 kW, and the design power level of 800 kW. These data indicate that more than 40 modes will likely need to be damped or otherwise defused in order to operate at 800 kW.

CONCLUSIONS

Parametric instabilities, studied in great depth and feared as a limitation to the attainable operating powers of interferometric gravitational wave detectors, have been observed for the first time in an Advanced LIGO detector. The behavior of the observed instability was found to be largely in agreement with models of the effect, implying that no significant ingredients have been omitted in the theoretical analysis.

Furthermore, the observed PI has been quenched by thermally tuning the optical resonance of the interferometer away from the resonance of the associated mechanical mode. This approach to PI, while sufficient for a small number of potentially unstable modes, may not be sufficient at higher operating powers where many modes are available for runaway excitation.

Thanks to many years of theoretical and experimental work on parametric instabilities, now informed by the observations described in this paper, the challenge faced by high-power interferometric gravitational wave detectors is clear and well understood. While the necessary mitigation techniques are not trivial, a suitable combination of thermal tuning, active damping of excited mechanical modes, and passive reduction of mechanical mode Q-factors is expected to be sufficient to allow Advanced LIGO to operate stably at full power.

The authors would like to acknowledge the extensive theoretical analysis of parametric instabilities by our Moscow State University colleagues Vladimir Braginsky, Sergey Strigin, and Sergey Vyatchanin, without which these instabilities would have come as a terrible surprise.

LIGO was constructed by the California Institute of Technology and Massachusetts Institute of Technology with funding from the National Science Foundation, and operates under cooperative agreement PHY-0757058. Advanced LIGO was built under award PHY-0823459. This paper carries LIGO Document Number LIGO-P1400254.

* mevans@ligo.mit.edu

[1] T. L. S. Collaboration, New Journal of Physics **11**, 073032 (2009).
[2] T. J. Kippenberg and K. J. Vahala, Optics Express **15**, 17172 (2007).
[3] T. J. Kippenberg and K. J. Vahala, Science **321**, 1172 (2008).
[4] D. McClelland, N. Mavalvala, Y. Chen, and R. Schnabel, Laser & Photonics Reviews , 677 (2011).
[5] M. Poot and H. S. J. van der Zant, Physics Reports **511**, 273 (2012).
[6] V. B. Braginsky, S. E. Strigin, and S. P. Vyatchanin, Physics Letters A **287**, 331 (2001).
[7] V. B. Braginsky, S. E. Strigin, and S. P. Vyatchanin, arXiv.org (2002), gr-qc/0209064v1.
[8] S. W. Schediwy, C. Zhao, L. Ju, and D. G. Blair, Classical and Quantum Gravity **21**, S1253 (2004).
[9] L. Ju, S. Grass, C. Zhao, J. Degallaix, and D. G. Blair, Journal of Physics: Conference Series **32**, 282 (2006).
[10] L. Ju, S. Gras, C. Zhao, J. Degallaix, and D. G. Blair, Physics Letters A **354**, 360 (2006).
[11] L. Ju, C. Zhao, S. Gras, J. Degallaix, D. G. Blair, J. Munch, and D. H. Reitze, Physics Letters A **355**, 419 (2006).
[12] A. G. Gurkovsky, S. E. Strigin, and S. P. Vyatchanin, Physics Letters A **362**, 91 (2007).
[13] S. E. Strigin and S. P. Vyatchanin, Physics Letters A **365**, 10 (2007).
[14] I. A. Polyakov and S. P. Vyatchanin, Physics Letters A **368**, 423 (2007).
[15] A. G. Gurkovsky and S. P. Vyatchanin, Physics Letters A **370**, 177 (2007).
[16] S. Schediwy, C. Zhao, L. Ju, D. Blair, and P. Willems, Physical Review A **77**, 013813 (2008).
[17] S. P. Vyatchanin and S. E. Strigin, Quantum Electronics **37**, 1097 (2008).
[18] C. Zhao, L. Ju, Y. Fan, S. Gras, B. Slagmolen, H. Miao, P. Barriga, D. Blair, D. Hosken, A. Brooks, P. Veitch, D. Mudge, and J. Munch, Physical Review A **78**, 023807 (2008).
[19] S. E. Strigin, D. G. Blair, S. Gras, and S. P. Vyatchanin, Physics Letters A **372**, 5727 (2008).
[20] S. E. Strigin, Physics Letters A **372**, 6305 (2008).
[21] H. Miao, C. Zhao, L. Ju, S. Gras, P. Barriga, Z. Zhang, and D. Blair, Physical Review A **78**, 063809 (2008).
[22] C. Zhao, L. Ju, H. Miao, S. Gras, Y. Fan, and D. Blair,

Physical Review Letters **102**, 243902 (2009).
[23] V. V. Meleshko, S. E. Strigin, and M. S. Yakymenko, Physics Letters A **373**, 3701 (2009).
[24] Z. Zhang, C. Zhao, L. Ju, and D. G. Blair, Physical Review A **81**, 013822 (2010).
[25] M. Evans, L. Barsotti, and P. Fritschel, Physics Letters A **374**, 665 (2010).
[26] S. E. Strigin and S. P. Vyatchanin, Physics Letters A **374**, 1101 (2010).
[27] S. E. Strigin, Optics and Spectroscopy **109**, 54 (2010).
[28] F. Liang, C. Zhao, S. Gras, L. Ju, and D. G. Blair, Journal of Physics: Conference Series **228**, 012025 (2010).
[29] S. Gras, C. Zhao, D. G. Blair, and L. Ju, Classical and Quantum Gravity **27**, 205019 (2010).
[30] S. E. Strigin and S. P. Vyatchanin, Gravitation and Cosmology **17**, 87 (2011).
[31] D. Heinert and S. E. Strigin, Physics Letters A **375**, 3804 (2011).
[32] S. E. Strigin, Optics and Spectroscopy **112**, 373 (2012).
[33] S. P. Vyatchanin and S. E. Strigin, Physics-Uspekhi **55**, 1115 (2013).
[34] S. L. Danilishin, S. P. Vyatchanin, D. G. Blair, J. Li, and C. Zhao, arXiv.org (2014), 1409.3284v3.
[35] X. Chen, C. Zhao, S. Danilishin, L. Ju, D. Blair, H. Wang, S. P. Vyatchanin, C. Molinelli, A. Kuhn, S. Gras, T. Briant, P. F. Cohadon, A. Heidmann, I. Roch-Jeune, R. Flaminio, C. Michel, and L. Pinard, arXiv.org (2014), 1411.3016v1.
[36] LIGO Laboratory, "LIGO web site," (living document).
[37] J. Degallaix, C. Zhao, L. Ju, and D. Blair, JOSA B **24**, 1336 (2007).
[38] L. Ju, D. G. Blair, C. Zhao, S. Gras, Z. Zhang, P. Barriga, H. Miao, Y. Fan, and L. Merrill, Classical and Quantum Gravity **26**, 015002 (2008).
[39] S. Gras, D. G. Blair, and L. Ju, Physics Letters A **372**, 1348 (2008).
[40] S. Gras, D. G. Blair, and C. Zhao, Classical and Quantum Gravity **26**, 135012 (2009).
[41] Y. Fan, L. Merrill, C. Zhao, L. Ju, D. Blair, B. Slagmolen, D. Hosken, A. Brooks, P. Veitch, and J. Munch, Classical and Quantum Gravity **27**, 084028 (2010).
[42] J. Miller, M. Evans, L. Barsotti, P. Fritschel, M. MacInnis, R. Mittleman, B. Shapiro, J. Soto, and C. Torrie, Physics Letters A **375**, 788 (2011).
[43] C. Zhao, L. Ju, Q. Fang, C. Blair, J. Qin, D. Blair, J. Degallaix, and H. Yamamoto, arXiv.org (2015), 1501.01542.
[44] S. Gras, C. Zhao, L. Ju, and D. G. Blair, Journal of Physics: Conference Series **32**, 251 (2006).
[45] Equation (9) in Evans 2010 is missing a factor of 2, resulting from a similar error in equation (24). This unfortunately matches a factor of 2 error in the equation for T in section 2 of Braginsky 2001, which should read $T = 4\pi L/(\lambda_0 Q_{opt})$, such that $\delta_1 = (c/2L)(2/T)$. Note that in Evans 2010 $G_n = 2/T$ for Braginsky's Fabry-Perot cavity on resonance (i.e., with $\Delta\omega_n = 0$).
[46] P. Fritschel, arXiv.org (2014), 1411.4547.
[47] S. Gras, P. Fritschel, and M. Evans, LIGO DCC (2015), P1400257.
[48] L. S. Collaboration and V. Collaboration, arXiv.org (2013), 1304.0670.